PHYSICAL REVIEW C **72**, 061305(R) (2005)

^{108}Sn studied with intermediate-energy Coulomb excitation

A. Banu,[1,2,*] J. Gerl,[1] C. Fahlander,[3] M. Górska,[1] H. Grawe,[1] T. R. Saito,[1] H.-J. Wollersheim,[1] E. Caurier,[4] T. Engeland,[5] A. Gniady,[4] M. Hjorth-Jensen,[5] F. Nowacki,[4] T. Beck,[1] F. Becker,[1] P. Bednarczyk,[1,6] M. A. Bentley,[7] A. Bürger,[8] F. Cristancho,[3,†] G. de Angelis,[9] Zs. Dombrádi,[10] P. Doornenbal,[1,11] H. Geissel,[1] J. Grębosz,[1,6] G. Hammond,[12,‡] M. Hellström,[1,§] J. Jolie,[11] I. Kojouharov,[1] N. Kurz,[1] R. Lozeva,[1,||] S. Mandal,[1,¶] N. Mărginean,[9] S. Muralithar,[1,**] J. Nyberg,[13] J. Pochodzalla,[2] W. Prokopowicz,[1,6] P. Reiter,[11] D. Rudolph,[3] C. Rusu,[9] N. Saito,[1] H. Schaffner,[1] D. Sohler,[10] H. Weick,[1] C. Wheldon,[1,††] and M. Winkler[1]

[1]*Gesellschaft für Schwerionenforschung (GSI), D-64291 Darmstadt, Germany*
[2]*Institut für Kernphysik, Universität Mainz, D-55099 Mainz, Germany*
[3]*Department of Physics, Lund University, S-22100 Lund, Sweden*
[4]*IReS, F-67037 Strasbourg Cedex 2, France*
[5]*Department of Physics and Center of Mathematics for Applications, University of Oslo, N-0316 Oslo, Norway*
[6]*The Henryk Niewodniczański Institute of Nuclear Physics, PAN, PL-31-342 Kraków, Poland*
[7]*Department of Physics, University of York, Heslington, York YO10 5DD, United Kingdom*
[8]*Helmholtz-Institut für Strahlen- und Kernphysik, Universität Bonn, D-53115 Bonn, Germany*
[9]*INFN Laboratori Nazionali di Legnaro, I-35020 Legnaro, Italy*
[10]*Institute of Nuclear Research of the Hungarian Academy of Sciences, H-4001 Debrecen, Hungary*
[11]*Institut für Kernphysik, Universität zu Köln, D-50937 Köln, Germany*
[12]*Department of Physics, University of Keele, Keele, Staffordshire ST5 5BG, United Kingdom*
[13]*Department of Radiation Sciences, Uppsala University, SE-75121 Uppsala, Sweden*

(Received 3 May 2005; published 29 December 2005)

The unstable neutron-deficient ^{108}Sn isotope has been studied in inverse kinematics by intermediate-energy Coulomb excitation using the RISING/FRS experimental setup at GSI. This is the highest Z nucleus studied so far with this method. Its reduced transition probability $B(E2;0^+_{\text{g.s.}} \rightarrow 2^+_1)$ has been measured for the first time. The extracted $B(E2)$ value of $0.230(57)e^2\,\text{b}^2$ has been determined relative to the known value in the stable ^{112}Sn isotope. The result is discussed in the framework of recent large-scale shell model calculations performed with realistic effective interactions. The roles of particle-hole excitations of the ^{100}Sn core and of the $Z = 50$ shell gap for the $E2$ polarization are investigated.

DOI: 10.1103/PhysRevC.72.061305 PACS number(s): 21.10.−k, 25.70.De, 23.20.Js, 21.60.Cs

The structure of nuclei far from β stability is currently a key topic of research, both experimentally and theoretically. Emphasis is put on phenomena such as shell evolution, proton-neutron interaction, and changes of collective properties. A burning question in nuclear structure physics is whether the shell closures known close to the valley of stability are preserved when approaching the limits of nuclear existence. Toward the proton drip line, because of the confinement of protons by the Coulomb barrier and/or the vicinity of the $N = Z$ line, changes in shell structure as well as collectivity are expected to be driven exclusively by the monopole drift [1–3] of single-particle states and the proton-neutron interaction between identical shell model orbitals [4]. Hence, core polarization studied in spin ($M1$, Gamow-Teller) and shape ($E2$) response, proton-neutron pairing, and isospin symmetry are appealing nuclear structure investigations. In this respect, the heaviest proton bound $N = Z$ doubly magic nucleus ^{100}Sn and its neighbors provide a principle test ground. Information on quadrupole polarization of the magic core can be inferred from the energy of the first excited 2^+ states and their $E2$ transition rates to the ground state. Experimentally, the nuclear properties of ^{100}Sn are only indirectly known [5–7], although its existence has already been confirmed [8,9].

The Sn isotopes between the $N = 50$ and 82 shell closures provide the longest chain of semi-magic nuclei accessible to nuclear structure studies, both in the neutron valence space of a full major shell and with emphasis on excitations of the $Z = 50$ core. The $B(E2;0^+_{\text{g.s.}} \rightarrow 2^+_1)$ value is most sensitive to details of shell structure and $E2$ core polarization. However, the existence of higher lying isomeric states in the tin isotopes hampers a direct measurement of the lifetime of the 2^+_1 states by standard Doppler methods (DSAM, RDM) and the very short lifetimes of the 2^+_1 states are not accessible to electronic timing methods. Therefore, a Coulomb excitation measurement is the only way to obtain this nuclear structure

*Present address: Cyclotron Institute, Texas A & M University, College Station, TX 77843, USA.
†On leave of absence from Universidad Nacional de Colombia, Bogota, Colombia.
‡Present address: Department of Physics, University of York, Heslington, York, UK.
§Present address: Department of Physics, Lund University, Lund, Sweden.
||Present address: Faculty of Physics, University of Sofia, Sofia, Bulgaria.
¶Present address: University of Delhi, New Delhi, India.
**Present address: Nuclear Science Center, New Delhi, India.
††Present address: Hahn-Meitner-Institut Berlin, Berlin, Germany.

information. Until recently only the $B(E2;0^+_{g.s.} \rightarrow 2^+_1)$ values of the stable $^{112-124}$Sn nuclei were measured in sub-barrier Coulomb excitation [10].

In the following, we report on the first intermediate-energy Coulomb excitation experiment performed on the ^{108,112}Sn isotopes using the RISING/FRS setup [11]. A primary beam of ^{124}Xe at 700 MeV/nucleon energy and an average intensity of 6×10^7 s^{-1}, delivered by the SIS accelerator at GSI, impinged on a 4 g/cm^2 ^{9}Be production target located at the entrance of the fragment separator (FRS) [12]. The Sn isotopes were produced via projectile fragmentation. Secondary beams were separated by the FRS operated in achromatic optics mode and identified on an event-by-event basis by coincidence measurements of energy loss in an ionization chamber, magnetic rigidity, and time of flight using two scintillator detectors. The trajectories of the projectiles were tracked with two multiwire proportional chambers. A wedge-shaped aluminium degrader with thickness of 4.59 g/cm^2 and 4.83 g/cm^2 for the ^{108}Sn and ^{112}Sn fragment settings, respectively, was placed at the middle focal plane of the FRS. This allowed an optimized separation of the fragments of interest, amounting in both cases to $\simeq$60% of the secondary beam cocktail. A secondary ^{197}Au target with a thickness of 386 mg/cm^2 was placed at the final focal plane of the fragment separator. The ^{108,112}Sn nuclei impinging on the gold target at 142 MeV/nucleon and 147 MeV/nucleon energies, respectively, were mainly excited by means of electromagnetic interaction. Gamma rays in coincidence with projectile residues were detected by the 15 RISING Ge-Cluster detectors [11,13]. The position-sensitive detector array CATE [14], consisting of 3 × 3 Si-CsI(Tl) modular ΔE-E telescopes, and covering an opening angle of 58 mrad, was placed 1426 mm downstream from the secondary target. It served for the reaction channel selection as well as for the scattering angle determination.

At intermediate energies, a Coulomb excitation measurement is an experimental challenge because of intense atomic background radiation and relativistic Doppler effects. Previously, the method has been applied to nuclei with $Z \leqslant 30$ only. The 15 RISING Ge-Cluster detectors were positioned at forward angles with a small opening angle of 3° (for each single crystal) to maximize the effective solid angle affected by the Lorentz boost, while at the same time minimizing the Doppler broadening. This allowed an energy resolution of 3% to be achieved for projectile residue velocities of $\cong$0.46c. To suppress the atomic background radiation, each Ge-Cluster detector was surrounded on the side by a lead sheet of 2 mm thickness, and its front face was shielded by a combination of Pb, Sn, and Al absorbers of 5 mm thickness. In the analysis, an add-back procedure (applied to all seven crystals within a Ge-Cluster) and a Doppler-shift correction were performed event by event. For technical reasons (see Ref. [15] for details) only five of the RISING Ge-Cluster detectors were suitable for the off-line data analysis. The top panel in Fig. 1 shows the Doppler-corrected energy spectrum of the excited ^{112}Sn, with the γ-ray line of interest at 1257 keV. The bottom panel shows the corresponding spectrum for ^{108}Sn with the γ-ray line at 1206 keV.

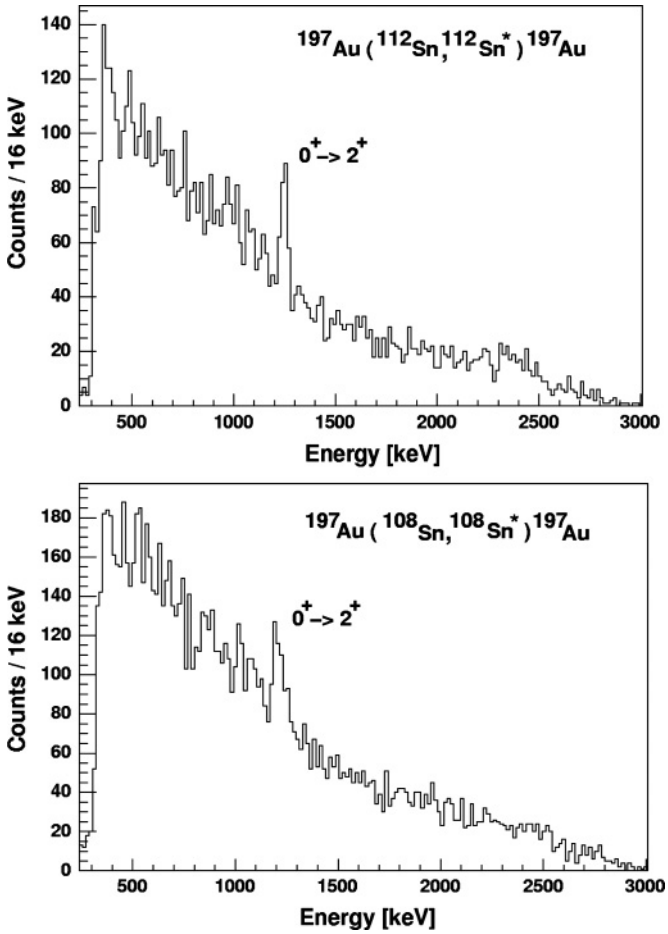

FIG. 1. De-excitation γ-ray lines following $0^+_{g.s.} \rightarrow 2^+_1$ Coulomb excitation of the ^{112,108}Sn projectiles, respectively.

The conditions applied in the data analysis to obtain the spectra in Fig. 1 are the following:

(i) fragment selection before the target with the FRS;
(ii) fragment selection after the target with CATE;
(iii) prompt γ time "window" (26 ns wide) selection;
(iv) Ge-Cluster multiplicity $M_\gamma(E_\gamma \geqslant 500\,\text{keV}) = 1$; and
(v) scattering angle selection between 1° and 2°.

Of the fragments selected in the FRS, about 80% of these events were tagged in CATE with 25% of these corresponding to Coulomb excitation and the rest to fragmentation reaction channels in the target. The intermediate-energy Coulomb excitation reaction is predominantly an *one-step process*, which implies a γ-hit multiplicity equal to one. However, it is possible that the de-excitation event is recorded in coincidence with background radiation originating from either atomic processes in the target or additional fragmentation reactions in the 1-cm-thick CATE-CsI detectors. In our case, owing to a small γ detection efficiency ($\lesssim$1%), only 3% of the recorded events correspond to a Ge-Cluster multiplicity greater than one. For an appropriate Coulomb excitation event selection, it was required in the analysis that the condition of single γ-hit cluster multiplicity is satisfied only for prompt γ rays at energies in

excess of 500 keV (in the laboratory frame), thus excluding nonsuppressed atomic radiation. The requested condition on the scattering angle (calculated in the laboratory frame) between 1° and 2° corresponds approximately to impact parameters in the range 11–22 fm [15]. Below this range one expects nuclear interactions to contribute, whereas above the elastic channel dominates with an increase in the electromagnetic radiation background. Further details on the optimization of the aforementioned conditions may be found in [15].

In spite of the strict data analysis, the spectra in Fig. 1 exhibit significant background even at energies around or above 1000 keV. This background is expected [11] to be manly created by fragmentation of the ^{108}Sn/^{112}Sn nuclei in the thick CATE-CsI detectors. The time resolution of the Ge-Clusters ($\simeq$14ns) is insufficient to disentangle it from γ rays emitted by fragments interacting with the gold target.

From the observation of the Doppler corrected γ line corresponding to the $0^+_{\text{g.s.}} \rightarrow 2^+_1$ transition in ^{108}Sn, the Coulomb excitation cross section can be extracted, which is directly proportional to the $B(E2)$ value [16]. In the analysis, effects such as particle-γ angular correlations, nuclear excitation, or excitations of higher lying 2^+ states (feeding contributions) have to be considered. These data are not available owing to limited statistics. Therefore, we present the experimental result of a relative measurement of the $B(E2; 0^+_{\text{g.s.}} \rightarrow 2^+_1)$ value in ^{108}Sn. The intermediate-energy Coulomb excitation measurement performed on ^{112}Sn with $B(E2; 0^+_{\text{g.s.}} \rightarrow 2^+_1) = 0.240(14)\ e^2\ \text{b}^2$ extracted from a subbarrier Coulomb excitation experiment [10] was used as normalization. This is justified since the two Coulomb excitation experiments were performed under very similar conditions [15]. The unknown feeding pattern is thus canceled out (assuming similar nuclear structure in both ^{108}Sn and ^{112}Sn as supported by theory), as well as the remaining nuclear contribution not removed by the scattering angle condition.

In Table I the experimental parameters needed to calculate the $B(E2)$ value in ^{108}Sn are listed. Additional information on data-taking time and the secondary beam intensity is given for both fragment settings.

The $B(E2; 0^+_{\text{g.s.}} \rightarrow 2^+_1)$ value in ^{108}Sn was determined as follows

$$B(E2\uparrow)_{108} = B(E2\uparrow)_{112} \times \frac{N_\gamma^{108}}{N_\gamma^{112}} \times \frac{N_p^{112}}{N_p^{108}} \times 0.88,$$

yielding $B(E2; 0^+_{\text{g.s.}} \rightarrow 2^+_1)_{108} = 0.230(57)\ e^2\,\text{b}^2$. The value 0.88 corresponds to the ratio of the proportionality factors between the excitation cross section and the reduced transition probability for ^{112}Sn and ^{108}Sn. The proportionality factors were calculated with the standard code DWEIKO [17] used for nuclear scattering at intermediate and high energies ($E_{\text{lab}} \geqslant 50$ MeV/nucleon), taking into account the scattering angle selection applied in the data analysis. Because the 2^+_1 excited states in ^{108,112}Sn lie close in energy, equal γ-ray efficiencies within experimental uncertainties were considered in the $B(E2)$ determination.

TABLE I. Photon yield N_γ, particle flux on target, N_p, data-taking time, and intensity (projectiles per second) for the two ^{108,112}Sn fragment settings.

Isotope	N_γ[a]	N_p[b]	Data-taking time	Intensity
^{108}Sn	174(26)	15×10^7	58 h	2480 Hz
^{112}Sn	106(20)	10×10^7	33 h	2400 Hz

[a]The photon yield was recorded with γ-particle trigger.
[b]The particle flux on target was inferred from down-scaled particle trigger (see Ref. [15]).

In the following, the measured $B(E2\uparrow)$ value in unstable ^{108}Sn is compared to the results of two large-scale shell model (LSSM) calculations. The first set of LSSM calculations was performed for the tin isotopes $^{102-130}$Sn, with a model space for neutrons consisting of the $1d_{5/2}$, $0g_{7/2}$, $1d_{3/2}$, $2s_{1/2}$, and $0h_{11/2}$ orbitals. Two sets of interactions with closed-shell cores ^{100}Sn and ^{132}Sn were considered, following the prescription outlined in Ref. [18] and using the CD-Bonn potential for the bare nucleon-nucleon interaction [19]. In the discussion here we focus however on the results obtained with the ^{100}Sn closed-shell core. A harmonic-oscillator basis was chosen for the single-particle wave functions, with an oscillator energy $\hbar\omega = 8.5$ MeV. The single-particle energies of the chosen model space orbits are $\epsilon_{1d_{5/2}} = 0.00$ MeV, $\epsilon_{0g_{7/2}} = 0.08$ MeV, $\epsilon_{1d_{3/2}} = 1.66$ MeV, $\epsilon_{2s_{1/2}} = 1.55$ MeV, and $\epsilon_{0h_{11/2}} = 3.55$ MeV. The neutron effective charge used in the calculations is $1.0e$. The results of the calculations for the energies of the 2^+_1 excited states and $B(E2; 0^+_{\text{g.s.}} \rightarrow 2^+_1)$ values are presented in columns 3 and 5 of Table II together with the experimental data measured recently for the unstable light isotope ^{108}Sn (this work), the unstable heavy isotopes ^{126,128,130}Sn [20], and the previously measured values for the stable isotopes $^{112-124}$Sn [10].

TABLE II. $I^\pi = 2^+$ energies and $E2$ strengths in $^{102-130}$Sn.

Isotope	$E_{2^+_1}$ [keV]		$B(E2\uparrow)[e^2\,\text{b}^2]$		
	Exp.[a]	SM[b]	Exp.	SM[b]	SM[c]
^{102}Sn	1472.0(2)	1647		0.043	0.044
^{104}Sn	1260.1(3)	1343		0.094	0.090
^{106}Sn	1207.7(5)	1231		0.137	0.125
^{108}Sn	1206.1(1)	1243	0.230(57)[d]	0.171	0.162
^{110}Sn	1211.9(2)	1259		0.192	0.192
^{112}Sn	1256.9(7)	1237	0.240(14)[a]	0.203	0.219
^{114}Sn	1299.9(7)	1208	0.24(5)[a]	0.209	0.235
^{116}Sn	1293.6(8)	1135	0.209(6)[a]	0.210	0.241
^{118}Sn	1229.7(2)	1068	0.209(8)[a]	0.208	0.239
^{120}Sn	1171.3(2)	1044	0.202(4)[a]	0.201	0.228
^{122}Sn	1140.6(3)	1076	0.192(4)[a]	0.184	0.206
^{124}Sn	1131.7(2)	1118	0.166(4)[a]	0.156	0.174
^{126}Sn	1141.2(4)	1214	0.10(3)[e]	0.118	0.134
^{128}Sn	1168.8(4)	1233	0.073(6)[e]	0.079	0.090
^{130}Sn	1121.3(5)	1191	0.023(5)[e]	0.042	0.047

[a]Ref. [10].
[b]LSSM in $\nu(g_{7/2}, d, s, h_{11/2})$ shell model space with ^{100}Sn closed-shell core and $e^\nu_{\text{eff}} = 1.0e$.
[c]LSSM in $\pi(g, d, s)$ and $\nu(g_{7/2}, d, s, h_{11/2})$ shell model space with ^{90}Zr closed-shell core and $e^\nu_{\text{eff}} = 0.5e$ (see text).
[d]This work.
[e]Ref. [20].

The comparison between experiment and theory shows agreement for the heavier Sn isotopes and in the case of ^{108}Sn within the error bars. However, a closer inspection of the light Sn isotopes reveals that part of the systematics seems to exceed the theoretical predictions. In the case of the interaction inferred for a ^{132}Sn core, the experimental $B(E2\uparrow)$ values are reproduced with effective charges between $0.7e$ and $0.8e$ [21]. This indicates a different character of core excitations in the $N = Z$ and $N > Z$ regions of the tin isotopic chain. Moreover, the effective charges for the lighter Sn isotopes show stronger renormalization effects, implying larger core polarization owing to particle-hole (ph) excitations.

To shed more light on the role of core-polarization effects, our second set of large-scale shell model calculations includes protons in the $0g_{9/2}$, $0g_{7/2}$, $1d_{5/2}$, $1d_{3/2}$, and $2s_{1/2}$ single-particle orbits as well, in addition to neutrons in the same model space as in the first set of calculations. The calculations allow up to 4p-4h proton core excitations (our computational limit), and the effective charges are set to the unscreened values $1.5e$ and $0.5e$ for protons and neutrons, respectively. Our closed-shell core is this time ^{90}Zr, and the effective interaction, derived along the same lines as was done previously and with the same nucleon-nucleon interaction, was, however, phenomenologically adjusted to the spectroscopy of Sn isotopes and $N = 82$ isotones; see Ref. [22] for more details. Because in this model space the *m*-scheme dimension [23] would be excessively large, the coupled code NATHAN [23] is used, which allows for a seniority truncation. Convergence was nearly obtained for seniority $v = 8$.

The experimentally observed asymmetry of the $B(E2)$ systematics, supported also by recent preliminary results on ^{110}Sn measured at REX-ISOLDE [24], suggests the importance of studying the role of proton core excitations and the evolution of the $Z = 50$ shell gap. The proton-neutron interaction, in particular the $\pi(0g_{9/2})-\nu(0g_{7/2}1d_{5/2}1d_{3/2}2s_{1/2})$ monopoles, responsible for the evolution of the spectroscopy between ^{91}Zr and ^{101}Sn, governs the evolution of the proton $Z = 50$ gap with the neutron filling. The tuning of the interaction for ^{91}Zr and ^{101}Sn is therefore sufficient to maintain the experimental $Z = 50$ shell gap as extracted from mass measurements. This is reflected in Fig. 2 for the proton effective single particle energies (ESPEs), as defined in Ref. [2], along the tin chain. Note that the ESPEs shown are not identical to the experimentally observed single-particle states that comprise configuration mixing. In particular, Fig. 2 shows the crossing for the ESPEs of the $1d_{5/2}$ and $0g_{7/2}$ orbitals owing to a strong $g_{7/2}-h_{11/2}$ proton-neutron monopole. An equally strong $g_{9/2}-h_{11/2}$ proton-neutron monopole is also needed to maintain a sufficiently closed ^{132}Sn core.

In Fig. 3 the experimental $B(E2)$ values [10,15,20] are compared to LSSM results for an increasing number $t = n$ of proton np-nh excitations. The evolutions of the $B(E2)$ systematics presented here from the pure neutron space to $t = 4$ proton excitations are very instructive: besides reflecting the number of interacting nucleons, the $t = 0$ curve shows a slight asymmetric maximum at $N = 70$, which is shifted to $N = 68$ ($t = 2$) and $N = 66$ ($t = 4$) with increasing number of ph excitations. It should be noticed that for the lightest Sn isotopes the calculations suffer from the strong assumptions

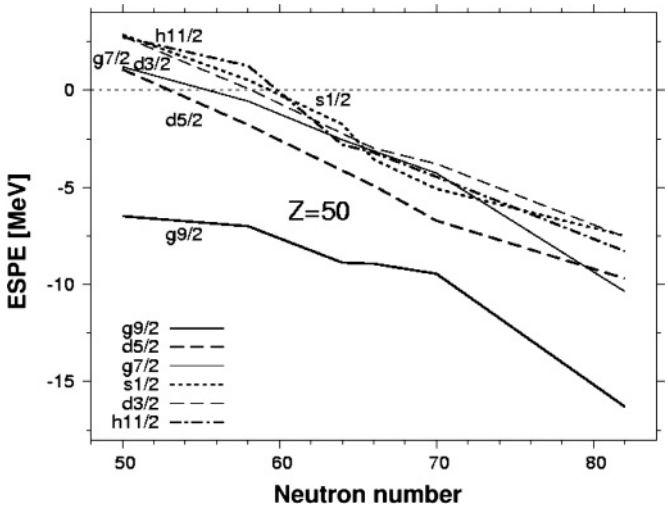

FIG. 2. Calculated evolution of the proton ESPE with the neutron number *N* along the chain of Sn isotopes.

of a $N = 50$ closure; thus the $B(E2)$ values for $^{102-106}$Sn are not fully trustworthy in our valence space. A gain of 15% in the $E2$ strength has been estimated for ^{106}Sn in the *gds* shell model space when both proton and neutron core excitations are allowed. It is also interesting to note that the untruncated 4p-4h proton core excitations ($t = 4gds$), with the corresponding $B(E2)$ values listed in the last column of Table II, show no increase but rather a small decrease in the $B(E2)$ strength for the heavy Sn isotopes in comparison to the $t = 4$ calculations truncated to the $0g_{9/2}$, $0g_{7/2}$, $1d_{5/2}$ orbitals, whereas for the light ones a substantial increase is observed. For the midshell and heavy Sn isotopes the $t = 4$ calculations seem to overestimate the $E2$ strength, which

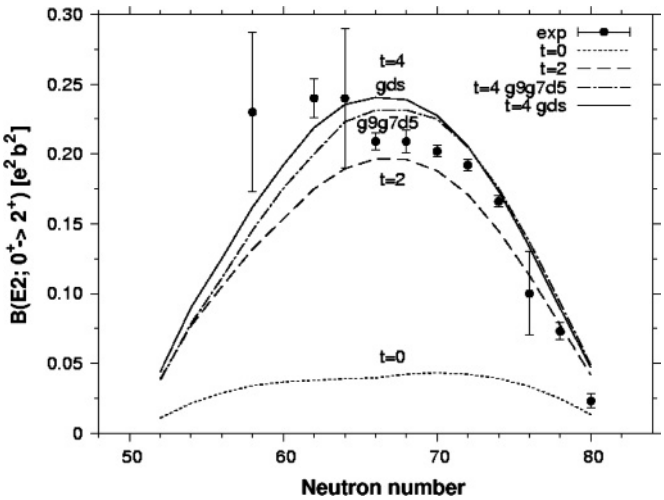

FIG. 3. Comparison of measured $B(E2\uparrow)$ values with LSSM predictions by taking into account ph core excitations. The $t = 0$ curve corresponds to calculations only for the valence neutrons as active particles. The $t = 2$ curve shows the major contribution as given by proton core excitations. The $t = 4$ curves are shown for the whole tin chain in a truncated proton model space and untruncated in the *gds* major shell.

can be ascribed to an ambiguity in the $\pi(0g_{9/2})-\nu(1h_{11/2})$ monopole owing to experimental uncertainties in the $11/2^-$ states of $N = 51$ isotones. A slight increase of the monopole contribution to the interaction would enlarge the $Z = 50$ shell gap in the heavier Sn isotopes and hence reduce the $B(E2)$ values. These calculations demonstrate the important role of core-polarization effects when one breaks the ^{100}Sn core and allows for proton excitations. Starting with the "canonical" neutron effective charge of $0.5e$, one clearly sees how the experimental $B(E2)$ values are reached when one allows for more proton ph excitations. Without these excitations and with neutrons only as degrees of freedom one would need neutron effective charges in the range of $(1-1.5)e$ to explain the experimental data. A more detailed discussion of these calculations will be presented in a forthcoming paper [22].

In conclusion, the $B(E2; 0^+_{\text{g.s.}} \rightarrow 2^+_1)$ value in the unstable ^{108}Sn isotope was measured for the first time by intermediate-energy Coulomb excitation. This is the highest Z nucleus studied with this method. The comparison with two different but complementary large-scale shell model calculations shows reasonable agreement with experiment and gives insight into the microscopic structure of the neutron $E2$ polarization charge. The evolution of proton ESPEs and the $Z = 50$ shell gap with increasing occupation of the $N = 50-82$ major shell governs the $E2$ correlations related to core polarization. The experimentally observed asymmetry can be traced back to enhanced polarization for light Sn isotopes at $t \geqslant 4$ proton ph excitations and/or to neutron core excitations across the $N = 50$ shell gap. The successful $B(E2)$ measurement on ^{108}Sn at GSI opens the research path to study with intermediate-energy Coulomb excitation the lighter Sn isotopes toward ^{100}Sn.

We thank the GSI accelerator staff for their efforts to produce a good-quality primary ^{124}Xe beam and the DVEE division at GSI for their support in data acquisition and Go4 software. This work was supported by the BMBF under Contract Nos. 06MZ176 and 06-K-167.

[1] P. Federman and S. Pittel Phys. Rev. C **20**, 820 (1979).
[2] T. Otsuka *et al*., Phys. Rev. Lett. **87**, 082502 (2001).
[3] H. Grawe, in *The Euroschool Lectures on Physics with Exotic Beams*, Vol. I, Lect. Notes Phys. **651** (Springer, Berlin Heidelberg, 2004), p. 33.
[4] A. Poves and A. P. Zuker, Phys. Rep. **70**, 235 (1981).
[5] M. Lipoglavsek *et al*., Phys. Lett. **B440**, 246 (1998).
[6] M. Górska *et al*., Phys. Rev. C **58**, 108 (1998).
[7] A. Blazhev *et al*., Phys. Rev. C **69**, 64304 (2004).
[8] M. Lewitowicz *et al*., Phys. Lett. **B332**, 20 (1994).
[9] R Schneider *et al*., Z. Phys. A **348**, 241 (1994).
[10] S. Raman, C. W. Nestor, and P. Tikkanen, At. Data Nucl. Data Tables **78**, 1 (2001).
[11] H. J. Wollersheim *et al*., Nucl. Instrum. Methods Phys. Res. A **537**, 637 (2005).
[12] H. Geissel *et al*., Nucl. Instrum. Methods Phys. Res. B **70**, 286 (1992).
[13] J. Simpson, Z. Phys. A **358**, 139 (1997).
[14] R. Lozeva *et al*., Acta Phys. Pol. B **36**, 1245 (2005).
[15] A. Banu, Ph.D. thesis, University of Mainz, 2005; http://archimed.uni-mainz.de
[16] A. Winther and K. Alder, Nucl. Phys. **A319**, 518 (1979).
[17] C. A. Bertulani, C. M. Campbell, and T. Glasmacher, Comput. Phys. Commun. **152**, 317 (2003).
[18] M. Hjorth-Jensen, T. T. S. Kuo, and E. Osnes, Phys. Rep. **261**, 125 (1995).
[19] R. Machleidt, F. Sammarruca, and Y. Song, Phys. Rev. C **53**, 1483(R) (1996).
[20] D. C. Radford *et al*., Nucl. Phys. **A746**, 83c (2004).
[21] A. Holt, T. Engeland, M. Hjorth-Jensen, and E. Osnes, Nucl. Phys. **A634**, 41 (1998).
[22] A. Gniady *et al*. (to be published).
[23] E. Caurier and G. Martínez-Pinedo, Nucl. Phys. **A704**, 60c (2002).
[24] J. Cederkäll *et al*. (to be published).